Symmetry of the phosphorus donor in diamond from first principles

Bozidar Butorac* and Alison Mainwood
Department of Physics, King's College London, Strand, London WC2R 2LS, United Kingdom
(Received 3 September 2008; published 16 December 2008)

Phosphorus is the only donor in diamond which can be used technologically. Several *ab initio* theoretical models have been published on substitutional phosphorus, and most of them have predicted that it should have tetrahedral or trigonal symmetry. Recent *ab initio* calculations suggested that C_{2v}, C_{3v}, and D_{2d} conformations reduce the total energy. Electron-paramagnetic-resonance experiments performed on phosphorus-doped diamond revealed a phosphorus-related center with tetragonal symmetry, although the signal is only observed below 20 K. We present a detailed *ab initio* study to show that the phosphorus substitutional atom has tetragonal symmetry at low temperatures. A study of the vibrational modes allows us to investigate the Jahn-Teller origin of the tetragonal distortion and to predict the solubility of phosphorus when grown by chemical vapor deposition with phosphine in the gas phase.

DOI: 10.1103/PhysRevB.78.235204 PACS number(s): 61.72.Bb

I. INTRODUCTION

One of the major obstacles in the development of diamond electronic devices has been the difficulty of finding a shallow donor. The obvious candidate, nitrogen, has a donor level at 1.7 eV,[1] which is much too deep to be used in electronics. The preparation of phosphorus-doped diamond by chemical vapor deposition (CVD), with phosphine in the gas phase, has only recently become reliable and reproducible. Homoepitaxial diamond thin films with thicknesses of about 300 nm were grown on the (111)-oriented faces of type Ib diamond substrates.[2] Over a wide range of dopant concentrations ($[PH_3]/[CH_4]$: 1000–20 000 ppm), the *n*-type conduction was confirmed by Hall-effect measurements. The concentration of phosphorus in the diamond can be controlled between 1×10^{16} and 5×10^{19} cm^{-3} by changing the PH_3/CH_4 ratio in the gas phase. Usually, 150 ppm of PH_3 with respect to CH_4 leads to a phosphorus concentration in the range of 1×10^{18} cm^{-3} depending on the growth conditions.[3] Other methods of doping, such as in diffusion and implantation, have had almost no success but this is a common situation for dopants in diamond. Since then, other source gasses, including tertiarybutylphosphine $TBP:P(C_4H_9)H_2$ and trimethylphosphine $TMP:P(CH_3)_3$, have been used to incorporate phosphorus.[4] However, its donor level at 0.6 eV is still very deep.[5–7]

Theoretical models of substitutional phosphorus[8–11] show a large outward distortion of the neighboring carbon atoms. The phosphorus itself either remains on site to give a tetrahedral defect[8,9] or distorts away from one of its carbon neighbors to give a trigonal symmetry[10] or conforms to C_{2v}, C_{3v}, and D_{2d} symmetries.[11] However, recent electron-paramagnetic-resonance (EPR) studies of P-doped diamond find a signal originating from a tetragonal defect, which disappears at temperatures above about 20 K.[12]

This paper reports on a study of the phosphorus donor to clarify the question of its symmetry, its solubility, and its electrical properties. It is arranged as follows. Section II explains the theoretical model that we used. Section III examines the structure, electrical properties, and solubility of the donor and we indicate why earlier models have given contradictory results. We conclude in Sec. IV.

II. METHOD

We used self-consistent density-functional theory (DFT) calculations using the SIESTA (Spanish Initiative for Electronic Simulations with Thousands of Atoms) package.[13] This code uses localized atomic numerical basis sets and periodic boundary conditions to describe valence electrons. Core electrons are treated by norm-conserving Troullier-Martins pseudopotentials[14] factorized in the Kleinman-Bylander form.[15] The generalized gradient approximation (GGA) was employed for the exchange-correlation potential, with the Perdew-Burke-Ernzerhof (PBE) parametrization of the exchange-correlation functional.[16] The carbon pseudopotential was nonrelativistic and the orbitals included were 2*s*, 2*p*, 3*d*, and 4*f*. The cutoff distances were all 1.25 bohr. The phosphorus pseudopotential was relativistic with 3*s*, 3*p*, 3*d*, and 4*f* orbitals. The cutoff distances for these channels were 1.58, 1.83, 1.83, and 1.83 bohr, respectively.

In all calculations the DZP (double zeta plus polarization orbitals) basis set was used. The energy cutoff was 350 Ry. Each system was allowed to undergo a full structural relaxation until the forces on atoms were smaller than 0.01 eV/Å. The stress tolerance was set to be less than 0.01 GPa. To find out how big the supercell of pure diamond needed to be, in order to represent a reliable bulk diamond, we calculated the energy per atom in supercells of 8, 16, 32, 64, 128, and 216 carbon atoms. We compared chemical potential of carbon obtained from these supercells with converged values of the chemical potential for carbon using two-atom supercell and 320 *k* points. It was found that chemical potential obtained from a 216-atom supercell with 1 *k* point is practically the same as the converged chemical potential obtained using two-atom supercell and 320 *k* points. It was found that supercells containing 64 or more atoms should be reliable. The lattice constant of bulk diamond we obtained using 216-atom supercell is 3.59 Å, overestimating the experimental value of 3.567 Å by only ~0.02 Å or 0.64%. The band gap is found to be 4.21 eV, underestimating the experimental band gap of 5.5 eV. This underestimate is a common problem of DFT. In our calculations, both 64- and 216-atom supercells were used.

One (gamma) k point was used in simulations. The structural optimization was performed using a conjugate gradient algorithm which means that during the structural relaxation, atoms are moved in a direction depending on both previous and current forces. This can have the disadvantage that the structure relaxes to a local minimum of the total-energy surface. So in order to ensure as much as possible that the relaxed structure is a true global minimum, we performed structural optimizations from several different initial configurations. We also let the supercell relax together with the atomic coordinates—this allows for a large outward relaxation of the carbon atoms around the big phosphorus atom where one might expect significant elastic strain in the lattice. This approach is slightly different from the one used by Sque *et al.*[17] where a supercell of fixed volume was employed.

III. RESULTS AND DISCUSSION

A. Structure and electric properties of the phosphorus donor

When the phosphorus in a 64-atom supercell is modeled with the spin averaged method, it relaxes into a tetragonal symmetry. The calculation was run with the starting positions of the atoms in tetrahedral and trigonal symmetries and with the neighboring atoms displaced in random directions from their sites, and in all cases the final symmetry was the same. This implies that there is no metastable structure of a different symmetry. Each of the first neighbors to the phosphorus relaxed outward by ~0.17 Å (11.1% of their bond length) and also by ~0.03 Å away from their tetrahedral positions. The spin-polarized calculation with the same 64-atom supercell gave a trigonal relaxation as the stable structure, again with no metastable structures.

However, when the calculations were repeated with a 216-atom supercell, using both spin-averaged and spin-polarized methods, the tetragonal structure with the displacements similar as above, where first neighbors to the phosphorus relaxed by ~0.02 Å away from their tetrahedral positions, was the one with lowest energy. The distances between four carbon atoms which surround phosphorus and their first neighbors shortened only slightly (two of them by 0.52% and the remaining one by 1.23%). This shows that distortion around P atom is much localized. The total energy in the tetragonal configuration is ~30 meV smaller than that of the trigonal structure for a 216-atom supercell. It is clear therefore that the structure predicted by the models is very sensitive to the supercell size, although we would expect that the larger supercell models would be more reliable. The relaxed structures showing the phosphorus atom and four nearest carbon atoms in D_{2d} and C_{3v} symmetries are given in Figs. 1 and 2, respectively.

Since there are three equivalent D_{2d} structures, it is possible for the system to hop from one of these configurations to either of the other two. In order to evaluate the potential barrier for reorientation we calculated the total energy of supercell in several consecutive configurations. In each of these configurations we fixed the positions of the P atom and four nearest C atoms and allowed the remaining atoms to relax in order to minimize the total energy. In this way we got a series of energy minima which enabled us to sketch the reorientation barrier along a particular migration path. Note that in each intermediate configuration phosphorus atom and four carbon atoms were fixed during simulations.

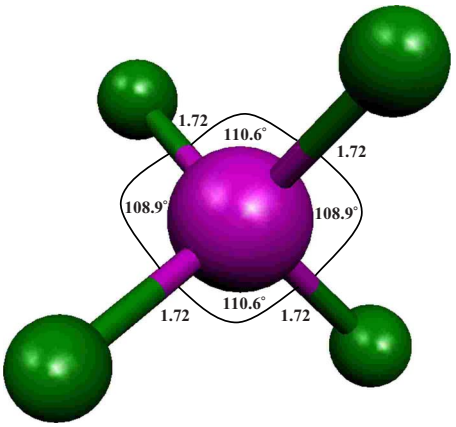

FIG. 1. (Color online) Relaxed P atom and its first neighbors in D_{2d} configuration for 216-atom supercell. Bond lengths are in angstroms. The vertical and horizontal axes are approximately [001] and [100], respectively.

One of the possible reorientation paths is via the T_d configuration and in this case the reorientation barrier is ~140 meV. In order to calculate this barrier we first found the P-C bond length for which the system has the lowest energy in T_d configuration.

The barrier on the direct path where each atom is halfway between two equivalent D_{2d} structures is ~70 meV. This barrier is shown in Fig. 3. The first point and last point in Fig. 3 correspond to two equivalent tetragonal structures and the point with the highest energy represents the saddle-point configuration. Note that since the phosphorus atom itself does not move during the reorientation, the reorientation paths are not totally clear. It is quite possible that a lower saddle-point energy exists.

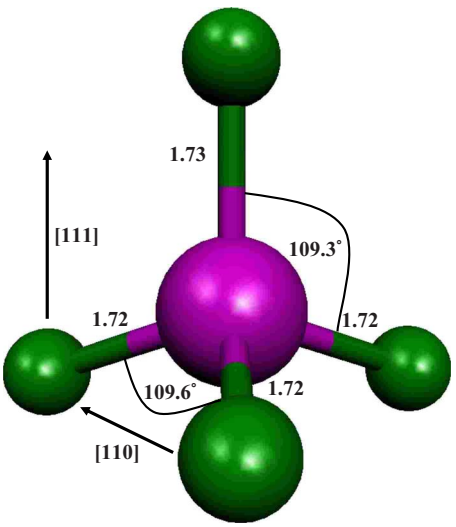

FIG. 2. (Color online) Relaxed P atom and its first neighbors in C_{3v} configuration for 216-atom supercell. Bond lengths are in angstroms.

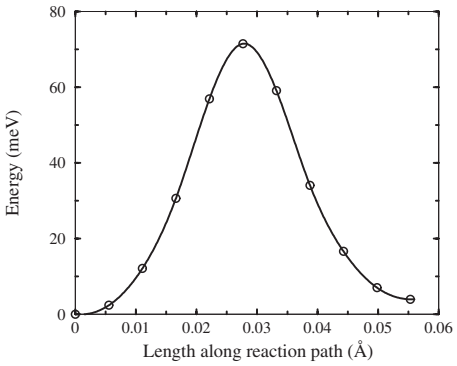

FIG. 3. Energy barrier for hopping between equivalent tetragonal structures. The horizontal axis represents the distance through which each of the four carbon atoms surrounding the phosphorus atom travels during the reorientation

We shall assume that rate of reorientation is of the form

$$R = \nu \exp(-E_a/kT), \tag{1}$$

where ν is an effective frequency and $\exp(-E_a/kT)$ is the probability of excitation over potential-energy barrier of height E_a. Note that this is a completely classical calculation. Quantum effects originating from the tunneling through the barrier can be neglected because the mass of the carbon atoms is too large to consider any tunneling. The effective frequency ν can be calculated as

$$\nu = \sqrt{\frac{1}{m}\frac{\prod_{i=1}^{3N} K_1(i)}{\prod_{j=1}^{3N-1} K_2(j)}}, \tag{2}$$

where $K_1(i)$ and $K_2(j)$ are the eigenvalues of the matrix of force constants in the minimum-energy structure and at the saddle point, respectively.[18]

In order to obtain the effective frequency, we calculated the phonon frequencies of the phosphorus containing supercell in the saddle-point configuration and at the tetragonal sites. The phonon spectra of the supercells were calculated using TETRA package.[19] The force-constant matrix (FCM) Φ is calculated by the method of finite displacements. This means that the atoms in the supercell are displaced by the small amounts u_i, then the forces on all atoms in the "displaced configurations" are calculated and these data are used to construct Φ. Two displacements, u_i and $-u_i$, are used for each degree of freedom. Using Eq. (2), the effective frequency for hopping is estimated to be about 2.6×10^{13} s^{-1}. For comparison, note that the Raman frequency is 4×10^{13} s^{-1}.

Our prediction of the temperature dependence of the EPR signal from the tetragonal phosphorus donor reveals that it starts to reorient rapidly at about 60 K. Therefore at low temperatures, the phosphorus can be expected to be observed in the tetragonal site, but at higher temperatures it will occupy a dynamic state which will be observed as tetrahedral or motion broadened so as to be unobservable.

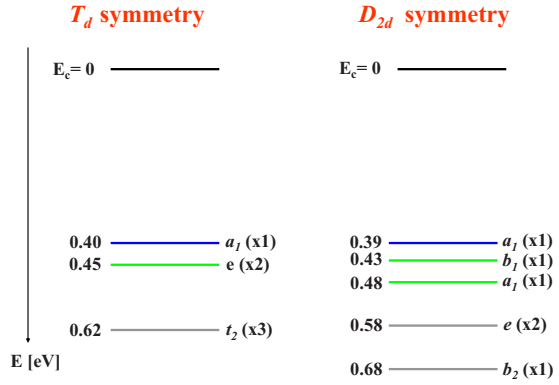

FIG. 4. (Color online) Kohn-Sham energy levels in the band gap when P is constrained to have tetrahedral symmetry and for lowest-energy (tetragonal) configuration.

The experimentally obtained temperature at which tetragonal EPR signal disappears is about 20 K.[12] The reason for this discrepancy is probably an overestimate of the height of the barrier. The exponential factor is dominant in the formula for reorientation, so even a slight overestimate of energy barrier can lead to big changes in the temperature dependence of the reorientation process.

In order to estimate the phosphorus donor level we used the Kohn-Sham energy levels, which are shown in Fig. 4. These levels can be interpreted as the ground state and the first few excited states of a phosphorus donor in diamond. They are effective-mass-like donor states which are derived from the minima of the conduction band.

B. Jahn-Teller effect

The relaxation from tetrahedral to a lower symmetry is due to a Jahn-Teller effect. When constrained to a tetrahedral symmetry, the Kohn-Sham energy level corresponding to the single donor electron has t_2 symmetry. In D_{2d} configuration this triply degenerate t_2 state is split into singly degenerate b_2 state which lies at 0.68 eV below the conduction-band minimum and a doubly degenerate E state. e and a_1 states in T_d configuration correspond to phosphorus excited states. We know that DFT is a ground-state theory and that Kohn-Sham eigenstates are not real electron wave functions but are actually a set of basis functions being used to find the charge density. Because of that, excited-state properties are beyond the reach of DFT and the positions of these excited phosphorus related levels have to be taken with caution.

Energies of t_2 and e states of the defect are plotted against the tetragonal distortion in Figs. 5(a) and 5(b). Note that the donor Kohn-Sham energy level is at 0.68 eV below the conduction-band edge. This is not a reliable estimate of the donor energy (cathodoluminiscence spectroscopy,[20] infrared-absorption spectroscopy,[21] and photoconductivity[5] show that donor levels is 0.6 eV below conduction band). The marker method is better to calculate donor or acceptor levels. Since the reference level for a donor in diamond is usually phosphorus we could not employ this method.

The change in the total energy of the defect is plotted against the tetragonal distortion in Fig. 5(c). From Figs.

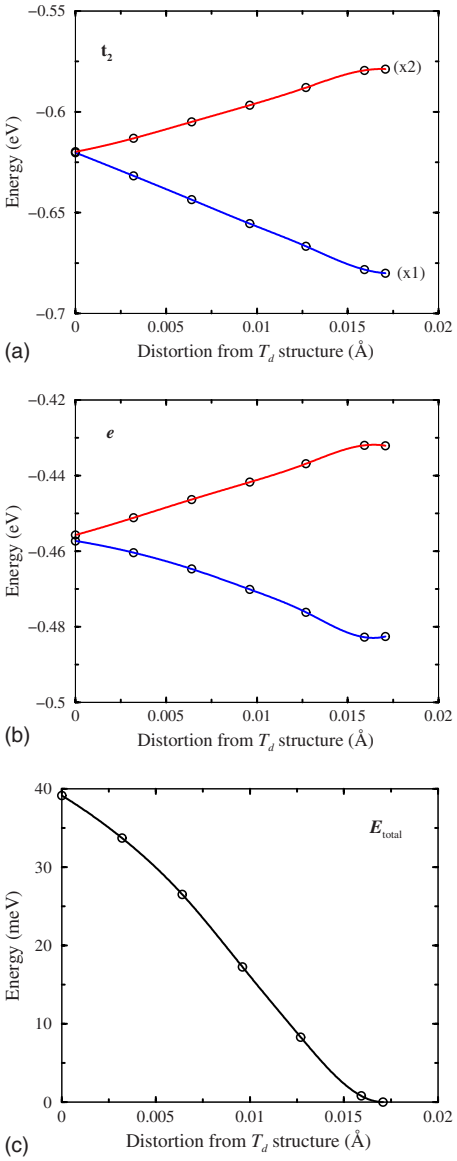

FIG. 5. (Color online) (a) Splitting of t_2 level as a function of distortion. The numbers in braces refer to the degeneracies of the levels. (b) Splitting of e level as a function of distortion. In (a) and (b) the zero of energy corresponds to the conduction-band minimum. (c) Decrease in the total energy of the defect as a function of distortion. In all figures, the coordinate 0 corresponds to T_d symmetry. The final point corresponds to the minimum-energy structure with D_{2d} symmetry.

5(a)–5(c) we can see that, as a consequence of increasing the magnitude of distortion, the energy of electronic states and the total energy continuously decrease. However, with the strain, the elastic energy is introduced and as this energy gets higher with the distortion it will eventually constrain the size of deformation. This is a classic example of a Jahn-Teller effect.

1. Coupling strengths

We concluded that, for this complex, we have $t_2 \times (\epsilon + \tau_2)$ coupling and we have analyzed the effect using the theory in Ref. 22. The ϵ mode tends to stabilize tetragonal distortion and τ_2 mode a trigonal distortion. One of the most interesting aspects of this situation is the competition of these two tendencies. We will assume that the coupling is linear. In that case, coupling to either of the vibrational modes is characterized by the linear coupling strengths which we shall denote as L_ϵ and L_τ. These quantities have the dimension of energy. Usually the magnitude of the vibronic coupling is expressed as a pure number,

$$S = \frac{1}{n}\frac{L^2}{(\hbar\omega)^2} \equiv \frac{E_{\mathrm{JT}}}{\hbar\omega}, \tag{3}$$

where $\hbar\omega$ is a vibrational quantum involved in coupling. The number n varies from case to case and is equal to 6 for $t_2 \times \epsilon$ and 9 for $t_2 \times \tau_2$. E_{JT} is the Jahn-Teller stabilization energy and S is a dimensionless linear Jahn-Teller coupling constant.[22]

Since the D_{2d} configuration is energetically more favorable than the C_{3v} configuration, we can conclude that

$$\frac{L_\epsilon^2}{6\hbar\omega} > \frac{L_\tau^2}{9\hbar\omega_\tau}. \tag{4}$$

In order to determine coupling strengths, we calculated vibrational modes for the 64-atom pure diamond supercell and for phosphorus containing supercell. The dynamical matrix has been obtained for both supercells. By diagonalizing these matrices, one can obtain phonon frequencies as explained above. This gives us 64×3 frequencies. From differences between the frequencies of the modes of vibration it is possible to identify those which involved the phosphorus. By analyzing normal coordinates, which were given in terms of atomic displacements, we could identify the frequencies of ϵ and τ_2 modes implicated in the Jahn-Teller effects as those of $\omega_\tau \sim 354$ cm^{-1} and $\omega_\epsilon \sim 586$ cm^{-1}.

To find the value of S_ϵ, we calculated vibronic levels in the case when $S_\epsilon \neq 0$ and $S_\tau = 0$. Using the fact that in our 216-atom simulations the difference between D_{2d} and T_d configurations was 40 meV, we read off the corresponding value of S_ϵ from Fig. 6. We found that S_ϵ is ~ 0.28. A similar procedure (Fig. 7) is used to find the value of S_τ and it is

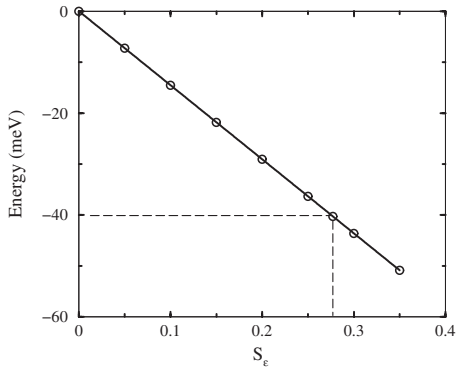

FIG. 6. Lowest-lying vibronic energy level as a function of coupling strength S_ϵ, while S_τ is zero.

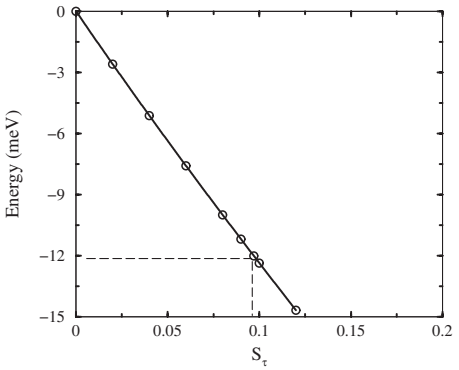

FIG. 7. Lowest-lying vibronic energy level as a function of coupling strength S_τ, while S_ϵ is zero.

found to be ~0.1. Here we used the result that the difference in energy between T_d and C_{3v} configurations is about ~12 meV for the 216-atom supercell.

Phosphorus is expected to behave as an effective-mass-like donor according to Ref. 6. It should therefore have a hydrogenic series of excited states. The Kohn-Sham eigenvectors, which can loosely be identified with wave functions, for the ground state and first-excited state are shown in Figs. 8 and 9. The localization of the wave functions shown in Figs. 8 and 9 compares well with that expected from the effective-mass-like theory explained in Ref. 6. However, the assumptions of effective-mass theory, in particular the use of the dielectric constant, break down when the wave functions are localized on just a few neighbors to the donor.

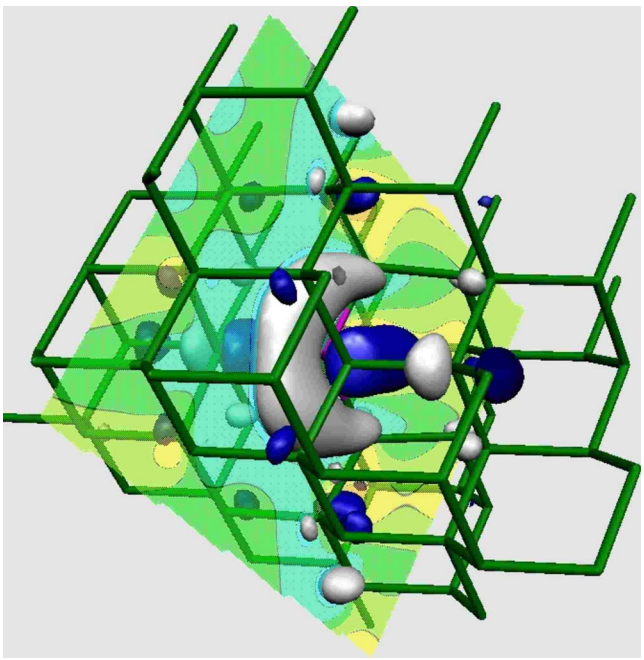

FIG. 8. (Color online) Isosurface plot for the highest occupied, t_2-derived orbital of the donor electron of the substitutional phosphorus in diamond, as sampled at the Γ point. Plot represents the wave function for the lowest of the three t_2-derived states in D_{2d} symmetry, which confirms that the orbital is localized around the P atom. It also shows σ_d reflection plane.

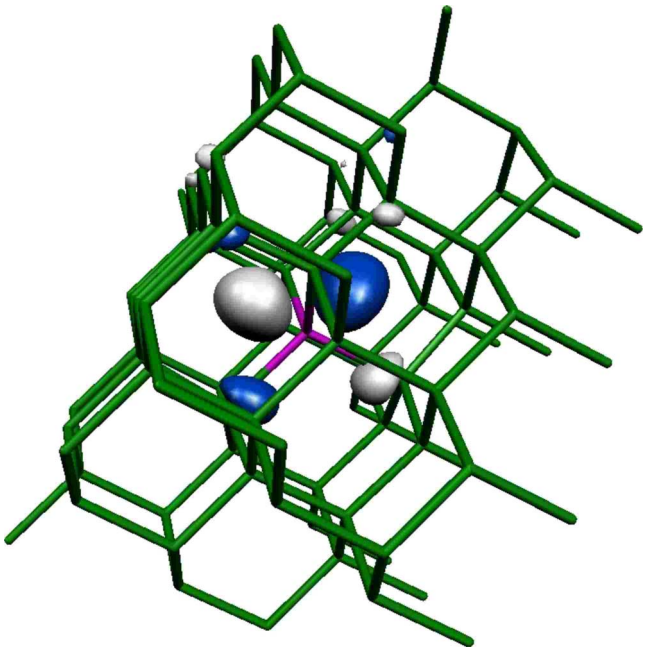

FIG. 9. (Color online) Isosurface plot for the orbital which represents one of the excited states of the donor electron of the substitutional phosphorus in diamond, as sampled at the Γ point. Plot represents the wave function for e orbital in D_{2d} symmetry.

We can see that the main component of the donor electron is on the phosphorus atom. The one-electron configuration of the on-site phosphorus in T_d symmetry is t_2^1. The lowering of symmetry from T_d to energetically most favorable D_{2d} symmetry causes splitting of t_2 level into b_2 and e. The wave function of b_2 level is related to sp hybrids pointing toward interstitial spaces in the diamond lattice.

The charge density along one of the P-C bonds when system has D_{2d} symmetry is given in Fig. 10. We also calculated the total charges inside the spheres of different radii centered at phosphorus atom. These data revealed that extra electron originating from phosphorus is localized around

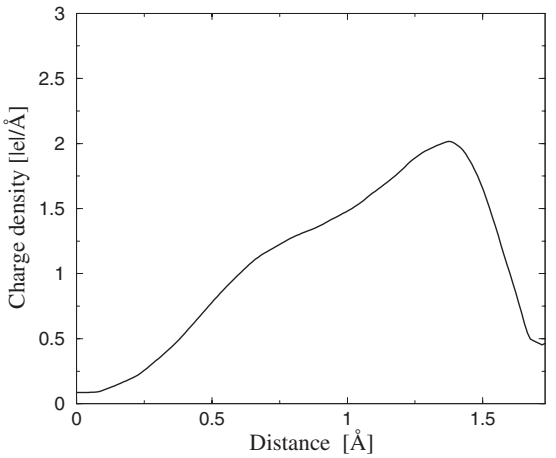

FIG. 10. Charge density along one of the P-C bonds when system has D_{2d} symmetry. The coordinate 0 Å corresponds to the center of P atom and the coordinate 1.73 Å is the center of the carbon atom.

TABLE I. Comparison of our results obtained for lattice parameter and zone-center phonons for C and Si with other theoretical and experimental data. Other theoretical data are from Ref. 25. The measured data are from Ref. 26.

	Lattice constant (Å)			Γ phonon (cm^{-1})		
	This work	Ref. 25	Expt.	This work	Ref. 25	Expt.
C	3.59	3.54	3.57	1386	1394	1332
Si	5.52	5.46	5.43	516	541	517

phosphorus atom and its four nearest carbon neighbors.

The stability of the different symmetries in these calculations depends on the supercell size. An additional factor in small supercells is the relaxation of supercell repeat distance. It proved possible to lock the symmetry into a trigonal or tetrahedral one by allowing only the atoms within the supercell to relax and fixing the repeat distance between supercells at the value for perfect diamond. Since the phosphorus atom is so much larger than the carbon atom, one would expect a dilation of the lattice if the concentration of phosphorus is as great as is being modeled (one atom in 64 or 216). This is probably the reason that other workers have reported conflicting results. Using standard elasticity theory,[23] we can calculate the elastic energy in the diamond corresponding to this dilation of the lattice around the phosphorus atom to be 0.16 eV.

C. Solubility of phosphorus

To calculate the solubility of phosphorus in diamond from phosphine, we have to equate the chemical potential of the solution with those of the phosphine gas and the diamond. For dilute solutions, the chemical potential is the Gibbs free energy per atom, $G=U-TS+pV$, in terms of the internal energy U, the entropy S, the pressure p, the volume V, and the temperature T. The internal energy of the dissolved phosphorus is the total energy of the supercell containing phosphorus less the total energy of the cell without the phosphorus plus the binding energy of the extra carbon atom displaced by the phosphorus. The entropy includes two terms: configurational (suffix con) and vibrational (suffix vib). Configurational entropy is given as

$$S_{\mathrm{con}} = -k_B \ln[P], \tag{5}$$

where $[P]$ is the concentration of phosphorus. The Helmholtz free energy is used to find the vibrational component of entropy. Working at constant volume can be justified since diamond has very small thermal-expansion coefficient of 10^{-6} K^{-1} at room temperature.

In the harmonic approximation, the Helmholtz free energy for a solid is given as[24]

$$F_{\mathrm{vib}}(T) = k_B T \int_0^\infty \ln[2 \sinh(\hbar\omega/2k_B T)] g(\omega) d\omega, \tag{6}$$

where k_B is the Boltzmann constant and $g(\omega)$ is the phonon density of states as a function of the frequencies ω. This integral extends up to the highest phonon modes which may include local defect modes. In the limit when $T \to 0$, F_{vib} gives the total zero-point energy (ZPE). The method used to calculate $g(\omega)$ from DFT results is shown in Ref. 25. The pV term is negligible for the solid or solution. The vibrational entropy can be calculated from F_{vib} by differentiation with respect to temperature,

$$S_{\mathrm{vib}} = -\left(\frac{\partial F_{\mathrm{vib}}}{\partial T}\right)_V. \tag{7}$$

After a little algebra the expression becomes

$$S_{\mathrm{vib}} = k_B \int_0^\infty \left\{ \frac{\hbar\omega}{2k_B T} \coth \frac{\hbar\omega}{2k_B T} - \ln\left(2 \sinh \frac{\hbar\omega}{2k_B T}\right) \right\} g(\omega) d\omega. \tag{8}$$

The chemical potential of the diamond solvent is calculated in the same way.

In order to obtain S_{vib}, it is necessary to know the vibrational frequencies. They were derived by diagonalizing the dynamical matrix of a 64-atom supercell representing bulk diamond and 64-atom supercell containing phosphorus atom as explained above.

To see how accurate our results are, we also calculated phonon frequencies for bulk silicon and diamond and compared our results with other theoretical and experimental data. The results are summarized in Table I.

The chemical potential of the phosphine gas can be calculated by assuming that it is an ideal gas, so that

$$S^{\mathrm{gas}} = k\left[\ln V + \frac{3}{2}\ln T + \frac{3}{2}\ln\left(\frac{2\pi m k_B}{h^2}\right) + \frac{5}{2}\right], \tag{9}$$

where m is the mass of the molecule. In addition, there are vibrational modes ω_i. For the polyatomic ideal gas, the vibrational entropy is[27]

$$S_{\mathrm{vib}}^{\mathrm{gas}} = N k_B \sum_{i=1}^{3n-6} \left\{ \frac{\beta\epsilon_i}{e^{\beta\epsilon_i} - 1} - \ln(1 - e^{-\beta\epsilon_i}) \right\}, \tag{10}$$

where N is the number of molecules, $\beta = 1/k_B T$, and $\epsilon_i = \hbar\omega_i$ are vibrational energy levels of the molecule. If a nonlinear molecule contains n atoms, there are $3n-6$ independent modes of vibration.

TABLE II. Calculated and measured (Ref. 28) vibrational frequencies for phosphine. Frequencies ν_2 and ν_4 are doubly degenerate. Units are in cm^{-1}.

	ν_1	ν_2	ν_3	ν_4
This work	1016.0	1087.4	2295.1	2331.9
Expt.	992.1	1118.3	2321.1	2326.9

The enthalpy and vibrational frequencies of the phosphine molecule can be calculated by DFT in the same way as those for diamond. The values of frequencies, compared to experiment, are given in Table II.

Once all this information is assembled, the equation can be rearranged to give an expression

$$[P] = \exp(\Delta S/k_B)\exp(\Delta E/k_B T), \tag{11}$$

where ΔS includes all the terms which derived from the differences in vibrational (and ideal gas) entropy between the solution and components and the pV term for the gas, and ΔE includes the similar enthalpy terms. During the growth of phosphorus-doped diamond, the pressure of the phosphine gas is simply its partial pressure in the gas mixture. Note that the entropy terms depend on temperature, so an analysis from an Arrhenius plot of the experimental values may be misleading.

However, the situation is complicated by the process by which diamond is grown. The gases are activated using a microwave plasma. This means that the components are unlikely to be in true equilibrium with each other at the temperature quoted as that of the substrate. Also the phosphine is probably dissociated in the plasma gas.

The solubility of phosphorus was calculated for a range of temperatures and for the following conditions: CH_4/H_2 ratio on the order of 0.05%, 100 ppm of phosphine with respect to CH_4, and gas pressure of 100 Torr. The results are summarized in Fig. 11. These values are within typical experimental conditions.[3] The solubility was also calculated for several values of phosphine with respect to CH_4 in the range of 1–1000 ppm and we found that solubility increases slightly with increasing phosphine concentrations.

Experimentally, the concentration of phosphorus in n-type CVD diamond can be controlled in the concentration range of 1×10^{16}–5×10^{19} cm^{-3} by varying the PH_3/CH_4 ratio in the gas phase.[3] Typically, 150 ppm of PH_3 with respect to CH_4 leads to a P concentration in the range of 10^{18} cm^{-3}, depending on the growth conditions. Therefore our results are in good agreement with experiment.

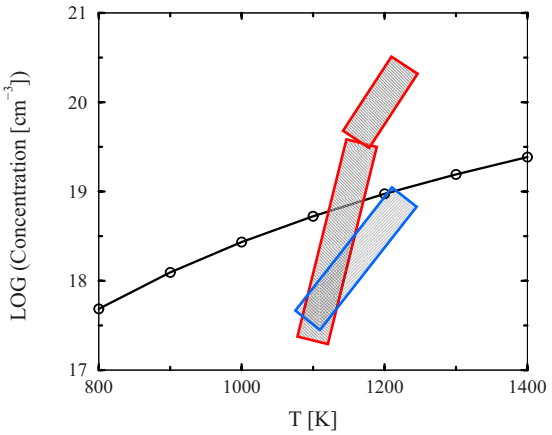

FIG. 11. (Color online) Black line: logarithm of the phosphorus concentration as a function of temperature for 100 ppm of phosphine with respect to CH_4 from our calculations. Red and blue blocks represent changes in phosphorus concentration in (111) and (001) CVD diamond, respectively, obtained experimentally in Ref. 4.

IV. CONCLUSIONS

In this paper, we studied the phosphorus donor to clarify the question of its symmetry and its solubility. It was found that configuration with D_{2d} symmetry has lower energy than the one with C_{3v} symmetry, which is in agreement with experiment. The energy barrier to reorient the defect is less than 70 meV. The relaxation from tetrahedral to a lower symmetry around the phosphorus atom is due to a Jahn-Teller effect. By calculating the phonon spectrum of a supercell containing phosphorus, we revealed which modes of vibration were coupling with the electronic levels of phosphorus. There is $t_2\times(\epsilon+\tau_2)$ coupling with modes of frequencies of $\omega_\tau\sim354$ cm^{-1} and $\omega_\epsilon\sim586$ cm^{-1}. The magnitudes of the vibronic coupling to these two vibrational modes are found to be $S_\tau=0.1$ and $S_\epsilon=0.28$.

The solubility of phosphorus in diamond from phosphine was also calculated. In the analysis we included the vibrational part of the internal energy and vibrational entropy. It was found that at the typical CVD growth temperatures the phosphorus concentration should be $\sim10^{19}$ cm^{-3}.

ACKNOWLEDGMENTS

We would like to thank the EPSRC-GB and the carbon-based electronics consortium for financial support for this work.

*bozidar.butorac@kcl.ac.uk

[1] R. G. Farrer, Solid State Commun. **7**, 685 (1969).
[2] S. Koizumi, M. Kamo, Y. Sato, H. Ozaki, and T. Inuzuka, Appl. Phys. Lett. **71**, 1065 (1997).
[3] M. Nesladek, Semicond. Sci. Technol. **20**, R19 (2005).
[4] H. Kato, T. Makino, S. Yamasaki, and H. Okushi, J. Phys. D **40**, 6189 (2007).
[5] M. Nesládek, K. Meykens, K. Haenen, L. M. Stals, T. Teraji, and S. Koizumi, Phys. Rev. B **59**, 14852 (1999).
[6] E. Gheeraert, S. Koizumi, T. Teraji, and H. Kanda, Solid State

Commun. **113**, 577 (2000).
[7] H. Kato, W. Futako, S. Yamasaki, and H. Okushi, Diamond Relat. Mater. **13**, 2117 (2004).
[8] K. Jackson, M. R. Pederson, and J. G. Harrison, Phys. Rev. B **41**, 12641 (1990).
[9] L. G. Wang and A. Zunger, Phys. Rev. B **66**, 161202(R) (2002).
[10] S. J. Sque, R. J. Jones, J. P. Goss, and P. R. Briddon, Phys. Rev. Lett. **92**, 017402 (2004).
[11] R. J. Eyre, J. P. Goss, P. R. Briddon, and J. P. Hagon, J. Phys.: Condens. Matter **17**, 5831 (2005).
[12] M. Katagiri, J. Isoya, S. Koizumi, and H. Kanda, Phys. Status Solidi A **201**, 2451 (2004).
[13] J. M. Soler, E. Artacho, J. D. Gale, A. Garcia, J. Junquera, P. Ordejon, and D. Sanchez-Portal, J. Phys.: Condens. Matter **14**, 2745 (2002).
[14] N. Troullier and J. L. Martins, Phys. Rev. B **43**, 1993 (1991).
[15] L. Kleinman and D. M. Bylander, Phys. Rev. Lett. **48**, 1425 (1982).
[16] J. P. Perdew, K. Burke, and M. Ernzerhof, Phys. Rev. Lett. **77**, 3865 (1996).
[17] S. J. Sque, R. Jones, J. P. Goss, and P. Briddon, Physica B **340-342**, 80 (2003).
[18] M. Lannoo and J. Bourgoin, *Point Defects in Semiconductors I* (Springer, New York, 1981).
[19] L. Kantorovich, LEV00 & TETR (2005).
[20] H. Sternschulte, K. Thonke, R. Sauer, and S. Koizumi, Phys. Rev. B **59**, 12924 (1999).
[21] E. Gheeraert, S. Koizumi, T. Teraji, H. Kanda, and M. Nesladek, Diamond Relat. Mater. **9**, 948 (2000).
[22] R. Englman, *The Jahn-Teller Effect in Molecules and Crystals* (Wiley-Interscience, London, 1972).
[23] *Solid State Physics, Advances in Research and Applications*, edited by F. Seitz and D. Turnbull (Academic Press, New York and London, 1956), Vol. 3.
[24] *Dynamical Properties of Solids*, edited by G. K. Horton and A. A. Maradudin (North-Holland, Amsterdam, 1974), Vol. 1.
[25] S. K. Estreicher, M. Sanati, D. West, and F. Ruymgaart, Phys. Rev. B **70**, 125209 (2004).
[26] http://www.ioffe.ru/SVA/NSM/Semicond/
[27] P. W. Atkins, *Physical Chemistry*, 5th ed. (Oxford University Press, New York, 1994).
[28] K. Rao, *Molecular Spectroscopy, Modern Research* (Academic, New York, 1976), Vol. 2.